



HAL
open science

The Phenomenology of West African Coastal Rainfall Events Based on a New Rain Gauge Network over Abidjan (Côte d'Ivoire)

Modeste Kacou, Eric-Pascal Zahiri, Kouakou Christian Yao, Luc Séguis, Clément Dutremble, Ehouman Serge Koffi, Jean Louis Perrin, Amidou Dao, Angah Armel Fourier Kodji, Kouamé Fréjus Konan, et al.

► **To cite this version:**

Modeste Kacou, Eric-Pascal Zahiri, Kouakou Christian Yao, Luc Séguis, Clément Dutremble, et al.. The Phenomenology of West African Coastal Rainfall Events Based on a New Rain Gauge Network over Abidjan (Côte d'Ivoire). *Atmosphere*, 2023, 14 (9), pp.1322. 10.3390/atmos14091322. hal-04876073

HAL Id: hal-04876073

<https://hal.science/hal-04876073v1>

Submitted on 9 Jan 2025

HAL is a multi-disciplinary open access archive for the deposit and dissemination of scientific research documents, whether they are published or not. The documents may come from teaching and research institutions in France or abroad, or from public or private research centers.




L'archive ouverte pluridisciplinaire **HAL**, est destinée au dépôt et à la diffusion de documents scientifiques de niveau recherche, publiés ou non, émanant des établissements d'enseignement et de recherche français ou étrangers, des laboratoires publics ou privés.



Distributed under a Creative Commons Attribution 4.0 International License

Article

The Phenomenology of West African Coastal Rainfall Events Based on a New Rain Gauge Network over Abidjan (Côte d'Ivoire)

Modeste Kacou ^{1,*}, Eric-Pascal Zahiri ¹, Kouakou Christian Yao ^{1,2}, Luc Séguis ^{1,2}, Clément Dutremble ², Ehouman Serge Koffi ³, Jean-Louis Perrin ², Amidou Dao ³, Angah Armel Fourier Kodji ¹, Kouamé Fréjus Konan ¹ and Kouassi Tandji Tewa ¹

- ¹ Laboratoire des Sciences de la Matière, de l'Environnement et de l'Energie Solaire (LASMES), Université Félix Houphouët-Boigny, Abidjan 22 BP 582, Côte d'Ivoire; eric.zahiri43@ufhb.edu.ci (E.-P.Z.); christian.yao@ird.fr (K.C.Y.); luc.seguis@ird.fr (L.S.); armelkodji@gmail.com (A.A.F.K.); konankouamefrejus97@gmail.com (K.F.K.); tewakouassitandji@gmail.com (K.T.T.)
- ² HydroSciences Montpellier (HSM), Institut de Recherche pour le Développement (IRD), Université de Montpellier, 34000 Montpellier, France; clement.dutremble@ird.fr (C.D.); jean-louis.perrin@ird.fr (J.-L.P.)
- ³ Laboratoire Géosciences et Environnement (LGE), Université Nangui Abrogoua, Abidjan 02 BP 801, Côte d'Ivoire; koffiserge.sge@univ-na.ci (E.S.K.); daoamidou.sge@univ-na.ci (A.D.)
- * Correspondence: modeste.kacou05@ufhb.edu.ci; Tel.: +225-0708090194



Citation: Kacou, M.; Zahiri, E.-P.; Yao, K.C.; Séguis, L.; Dutremble, C.; Koffi, E.S.; Perrin, J.-L.; Dao, A.; Kodji, A.A.F.; Konan, K.F.; et al. The Phenomenology of West African Coastal Rainfall Events Based on a New Rain Gauge Network over Abidjan (Côte d'Ivoire). *Atmosphere* **2023**, *14*, 1322. <https://doi.org/10.3390/atmos14091322>

Academic Editors: Isaac Nooni, Daniel Fiifi Tawia Hagan, William Amponsah, Nana Agyemang Prempeh and Benjamin Lamptey

Received: 14 June 2023

Revised: 20 July 2023

Accepted: 23 July 2023

Published: 22 August 2023



Copyright: © 2023 by the authors. Licensee MDPI, Basel, Switzerland. This article is an open access article distributed under the terms and conditions of the Creative Commons Attribution (CC BY) license (<https://creativecommons.org/licenses/by/4.0/>).

Abstract: In the District of Abidjan, flooding typically occurs suddenly during intense rainfall events. The individual rainfall event provides the basic element for the study. Its analysis is required to develop solutions for managing the impact of extreme rainfall occurrences. Our study proposes to identify individual rainfall events that occurred in the District of Abidjan from a densified network and analyze some of their characteristics related to the amount of rainfall they provided, their duration, and their level of intensity. A total of 1240 individual rainfall events were identified between 2018 and 2021 using a network of 21 rain gauges. Rainfall events were identified based on criteria such as a minimum inter-event time without rainfall of 30 min, a detection threshold of 0.02 mm/5 min, a minimum duration of 30 min applicable to the average hyetograph, and a minimum of 1 mm of rainfall in at least one rain gauge. The analysis of characteristics related to accumulation, intensity, and duration showed that the rainfall events were essentially convective, with an average duration of more than 2 h and a rainfall of 11.30 mm/event. For 70% of the rainfall events of a mixed nature, the convective episodes last up to 33.33% of the total duration of the event and produce an average of 80% of the cumulative rainfall. The 30-min peak intensities generally occur in the first half of the event. Less than 13.5% of the events have peaks greater than 50 mm/h. The probability of observing more than two, three, or four events per day is high in June and October, the core of the two rainy seasons.

Keywords: rainfall event identification; convective spells; rainfall intensity; I30max; Abidjan

1. Introduction

Rainfall plays two important roles. First, it plays a role in the development of life because it is the main source of fresh water [1,2]. Second, abundant rainfall can be a source of distress and cause the loss of life through flooding and landslides. Conversely, scarcity of rainfall can cause droughts, which also pose significant challenges. Furthermore, there are other hydrometeorological risks to consider [3]. Indeed, an excess or a deficit of rainfall may have negative consequences, especially for West African countries. A large part of their economy depends on rainfall, and they are less resilient to hydro-climatic disasters. For at least two decades, these countries have faced recurrent floods and droughts [4]. In general, in the tropics, rainfall is associated with convective systems, which are sometimes violent.

Thunderstorms constitute these convective systems that, due to the violence of the wind gusts and the associated torrential rains, can be the cause of flooding disasters. Unlike the Sahel, where convective systems are more organized [5], these cloud clusters appear less organized at the Gulf of Guinea [6]. It is this type of cloud cluster that is associated with the flooding, which confronts in West African cities, especially in the District of Abidjan (Côte d'Ivoire). In fact, according to statistics, there have been an average of 13 rainfall-related deaths every year since 2009 in the city of Abidjan [7]. Moreover, Abidjan's topography is just as prone to flooding. The city is dominated by two landforms: the plains and plateaus. The plains, which are generally found in the south (39% of the city's area), are characterized by altitudes at sea level (between 0 and 14 m) and are not conducive to run-off. In contrast, in the north, there are low and high plateaus representing 61% of the city's area, with altitudes between 30 and 140 m. The further from the coast, the higher the altitude is. In these plateau areas, the valleys that serve as natural drainage channels for rainwater are urbanized [8,9]. This terrain makes the city of Abidjan an area prone to flooding. According to a report by the Office for the Coordination of Humanitarian Affairs [7], 26% of the city of Abidjan is made up of areas at risk of flooding or landslides.

In general, precipitations, which result from complex atmospheric processes, are highly variable in both time and space. Analysis over timeframes longer than 24 h do not allow for the capture of individual characteristics of each rainfall event. As a consequence, phenomena such as flash floods that arise, at times, within a few minutes or hours after intense rainfall are not fully explicated. According to Peters and Christensen [10], the basic element facilitating an analysis of rainfall characteristics is the rainfall event. However, based on the complex nature of rainfall events, the definition of a rainfall event is not straightforward [11].

Yen and Chow [12] listed five definitions associated with rainfall events. This is in line with the variety of identification methods that exist in the literature [13]. Among these various methods and definitions, the most common definition of a rainfall event is a continuous period of rainfall that may include non-rainy periods. However, the duration of a non-rainy period cannot exceed the minimum duration between two distinct consecutive rainfall events, the minimum inter-event time (MIT). Additionally, a rainfall event is associated with a minimum amount of rainfall [14]. However, the criteria for choosing the MIT are not consistent. Indeed, in his review of the literature, Dunkerley [14] found several MIT values between 3 min and 24 h, as well as minimum accumulations between 0.2 and 13 mm. The value chosen depends on the study objectives and on the temporal resolution of the rainfall data. In order to analyze the temporal dynamics of rainfall events during the flood season, Wang [15] suggested a MIT of 6 h, a minimum event duration of 3 h, and a minimum accumulation of 10 mm. Sottile et al. [16] considered an MIT of 1 h and a cumulative threshold of 1 mm. Terranova and Gariano [17] considered an MIT of 6 h so that the hydrological impact (in terms of runoff) of two rainfall events could not be superimposed. Joo et al. [18] and Nojumuddin et al. [19] analyzed statistical methods based on the autocorrelation or coefficient of variability coupled with the characteristics of urban basins to determine the optimal MIT. The choice of an MIT is more related to hydrological considerations rather than to the physical and meteorological properties of rainfall [20]. However, the MIT method is simple to implement, hence its widespread use [14,15,21–25] and its adoption in our study.

In this study, we focus on the rain generated by convective systems. However, one of the major difficulties in studying rainfall event characteristics is the lack of reliable data. In Abidjan, until very recently, the only functional rain gauge that existed was the rain gauge located at the airport in the southeastern part of the city. This rain gauge belongs to the Direction de la Météorologie Nationale. This makes it impossible to carry out analyses that took account both of the spatial and temporal nature of rainfall events. Following on the Aghien project (2015–2018, <http://www.laguneaghien.org/> (accessed on 15 February 2023)), the EVIDENCE project (2018–2023, <http://www.evidence-ci.org/> (accessed on 15 February 2023)), which aims to help to reduce the risks associated with extreme rainfall

events impacting urban populations' living conditions, a unique opportunity has arisen to address the lack of measurement data. During these projects, 21 rain gauges have been strategically distributed across the urbanized area of the district to gather essential rainfall data. The aim of this study is to identify and characterize the various rainfall events that occurred in Abidjan's district from a densified network of rain gauges in the urban area using data collected from 2017 to 2022. This is one of the first networks of such density deployed in urban areas on the coast of the Gulf of Guinea. This study provides additional knowledge on the characteristics of rainfall events in an equatorial climate, which serves as a basis for other types of analysis such as numerical modeling, nowcasting, and, especially for engineers in the construction of design rainfalls for flood protection, structures and other water management strategies.

2. The Study Area, Data, and Methods

2.1. The Study Area

The study area is the district of Abidjan with an area of 2119 km². Its urbanized section was equipped with a network of rain gauges (Figure 1). It is located on the coast of the Gulf of Guinea between latitudes 5.23° N and 5.60° N and longitudes −4.46° W and −3.71° W. Its tropical climate is hot and humid with four seasons regulated by the West African monsoon. In a recent article, the Direction de la Météorologie Nationale (National Weather Service) indicated the following seasons: the long dry season from December to March, the long rainy season from April to July, the short dry season from August to September, and the short rainy season from October to November [26].

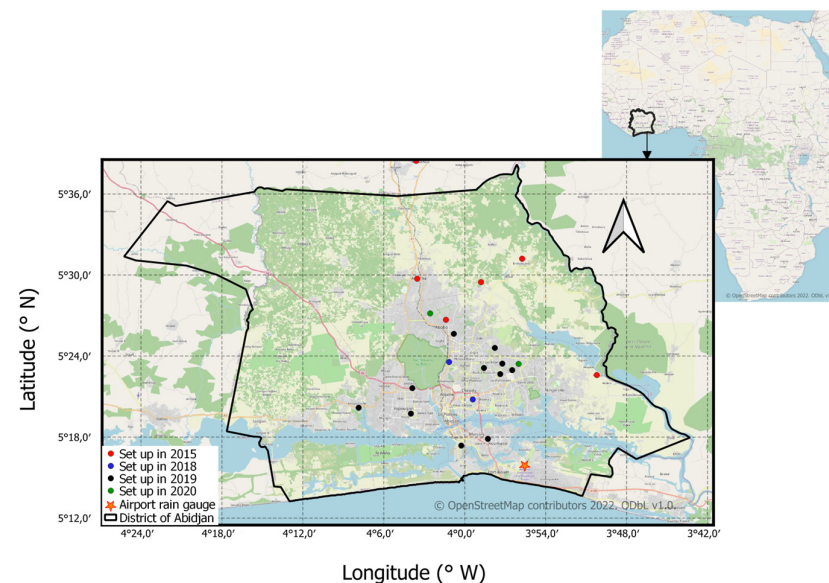


Figure 1. The study area and ground measurement system composed of rain gauges marked by dots.

2.2. Data

Through this study, we analyzed rainfall data from a research network of 21 rain gauges installed between 2015 and 2020, as can be seen in Figure 1 and in Table 1 [27]. The network is mainly deployed in the urbanized part of the district (representing roughly a box of 30 km × 40 km) with an average distance between rain gauges of 14.2 km. The minimum and maximum distances between rain gauges are 1.2 km and 39.6 km, respectively. Half of the rain gauges in the network have an inter-distance of less than 5 km. This relatively high density makes the network unique in an urban environment, particularly in sub-Saharan Africa. Rainfall is recorded with the same model of *Precis Mécanique*[®] tipping bucket rain gauges calibrated at 0.5 mm (Figure 2). The interception cone located at 1.5 m from the ground has a surface of 400 cm². The rain that has passed through the rain gauge is collected in a totalizing can at the foot of the apparatus. The tipping dates of the buckets

(day, month, year, hour, minute, and second) are recorded in a HOBO Pendant® data logger and then collected and reviewed monthly. After a critique and comparison with the totalizer, the tipping dates are aggregated in regular 5-min time steps. When a rain gauge malfunctions, its data are put into gaps over the identified period, and the values are replaced by NAN (not a number). In practice, the data we used in the present study are spread over four years from 7 January 2018 to 31 December 2021 to consider year from which we start densification of the network. In addition, before 2018, the network operation was not optimal, with many gaps at some stations. The data are available in the ORIESA database and identified with the DOI: <https://doi.org/10.23708/JOE1X6>. Thirteen (13) of these rain gauges are equipped with a remote transmission system. The data are processed and displayed on a map of the city, showing rainfall totals over the last 5 min up to the previous 3 days. The maps can be viewed in real time at <http://www.babiplus.org/> (accessed on 20 February 2023) and are updated every 5 min.

Table 1. The 21 rain gauges stations constituting research network set up during Aghien and EVIDENCE projects. Stations are listed in order of their installation year.

Number	Name	Longitude (°W)	Latitude (°N)	Year of Installation
1	Azaguié	4°3'36.792''	5°38' 27.492''	2015
2	Brofodoumé	3°55'44.904''	5° 31'12.612''	2015
3	Achokoi	3°50'12.624''	5°22'35.508''	2015
4	Attiekoi CET	3°58'47.604''	5°29'28.392''	2015
5	Anyama	4°3'31.608''	5°29'43.584''	2015
6	Ste Foi	4°1'23.628''	5°26'40.956''	2015
7	UNA	4°1'9.732''	5°23'33.216''	2018
8	UFHB	3°59'24.324''	5°20'47.004''	2018
9	Riviera Nord F9	3°56'28.932''	5°22'57.36''	2019
10	Riviera centre F12	3°58'34.608''	5°23'6.936''	2019
11	Djibi F3	3°57'46.224''	5°24'36.036''	2019
12	Adiopodoumé	4°7'52.068''	5°20'10.176''	2019
13	INFAS	4°0'15.48''	5°17'21.912''	2019
14	Yopougon Usine	4°3'53.316''	5°21'37.332''	2019
15	Marcory	3°58'17.004''	5°17'51.9''	2019
16	Yopougon CNPS	4°3'59.688''	5°19'44.04''	2019
17	UNA CFC	4°0'48.636''	5°25'38.676''	2019
18	Notre Dame	3°57'22.14''	5°22'39.684''	2019
19	Beraca	3°57'12.996''	5°23'26.232''	2019
20	Abobo Bois sec	4°2'34.008''	5°27'9.468''	2020
21	Cité Sir	3°56'0.564''	5°23'24.936''	2020

2.3. Methods

2.3.1. Rainfall Event Definition

Considering the small spatial extension and the relative density of our network (1 rain gauge/60 km² on the urbanized part and 1 rain gauge/100 km² at the district scale), we adopted a rainfall event definition that is similar to Löwe et al. [24]. This definition is mainly based on the criteria of the intensity threshold, minimum inter-event duration (MIT), and rainfall event duration. In their approach, Löwe et al. [24] considered a minimum intensity threshold of at least 0.02 mm/min at a rain gauge for the detection of rainfall events. The end of the event is determined when no rainfall greater than or equal to this intensity is observed on the rain gauge network for at least 1 h, which is their MIT. Finally, they considered a third criterion, which is related to the minimum duration of a rainfall event. This approach allowed us to use our network and work in urban areas.



Figure 2. A Precis Mécanique[®] tipping bucket rain gauge equipped with a remote transmission system. The top of the rain gauge is 1.5 m above the ground, in accordance with WMO standards. The green can, buried between the two tires, is the totalizer used to check that the tilts correspond to the amount of rain collected. The mast on the left carries the solar panel used to recharge the battery of the remote transmission system. The rain gauge reference from Precis Mécanique[®] is model 3039 resolution 0.5 mm (untouchable, extended range 0–1000 mm/h). Patented mechanical system 1154024/400 cm² cone.

In our study, we first determined the average hyetograph on the network by calculating the average rainfall at each time step. Subsequently, on the basis of the time series thus obtained, we proceeded to the splitting of the rainfall events by considering a threshold of average accumulation of detection fixed at 0.02 mm/5 min and an MIT of 30 min. This approach based on the use of the whole network allowed us to integrate the spatial variability, as well as the temporal dynamics, of rainfall in our analysis.

The threshold of 0.02 mm allowed us to consider events that were observed by only a small number of rain gauges. We could thus consider events observed at the edge of the network or by only one rain gauge. Therefore, the choice of an MIT of 30 min to distinguish two consecutive events appears suitable. It takes into account both the temporal resolution of our data and the climatic environment of the study area. In the district of Abidjan, rainfall events are dominated by thunderstorms and monsoon rains [28]. These meteorological conditions can lead to consecutive rainfall events that differ in their meteorological characteristics. Our value of MIT is identical to the 30 min used by Kouamé [29] in the northwest of the Côte d’Ivoire under a Sudanian climate, and by D’amato and Lebel [30] over the square degree of Niamey in Niger under a Sahelian climate, which is drier.

This study used the drawre function of the IETD library [31] of the R software version 3.6.2 [32], which allows for the identification of the beginning, end, duration, average intensity, and rainfall amount of the different rainfall events from the average hyetograph. Based on this information, the event rainfall amount at each rain gauge was computed. In a final step, we identified the events that lasted at least 30 min with a minimum rainfall amount of 1 mm observed in at least one rain gauge of the network. This approach ensures that only significant rainfall events are considered for further analysis.

In summary, a rainfall event was defined if it lasted at least 30 min over the entire network with a minimum accumulation of 1 mm observed on at least one rain gauge, and with a dry period of at least 30 min separating it from the next event.

2.3.2. Convective/Stratiform Separation

Once the rainfall events are identified, the next step is to determine their convective or stratiform nature. To do this, we classified rainfall intensity time series as convective or stratiform by adapting the classification method of Testud et al. [33]. They classify an intensity R at Time Step i (R_i) as stratiform if, and only if, R_i and its 10 adjacent values (from R_{i-5} to R_{i+5}) are all less than 10 mm/h. If not, R_i is classified as convective. This classification was applied over northern Benin by considering 20 adjacent values on a one-minute rain intensity time series [34]. In addition to the threshold, some authors used standard deviation for their stratiform convective classification with an intensity threshold of 5 mm/h and a standard deviation of 1.5 mm/h [35,36] with a one-minute time series.

In our study, the methodology of Testud et al. [33] and Moumouni et al. [34] was adapted, but considering only the two adjacent values, i.e., R_{i-1} , R_i and R_{i+1} , in order to consider the coarser temporal resolution of our data (5 min). Finally, we used the same intensity threshold of 10 mm/h as already applied in the region by Moumouni et al. [34]. This classification was applied at the static level, i.e., at each rain gauge and for each rainfall event defined on the mean hyetograph reading.

Thus, a rainfall event is classified convective if all the rain intensities at all the rain gauges are identified as convective. If the intensities are all classified as stratiform, the event is categorized as stratiform. On the other hand, if the event exhibits both types of rainfall, it is classified as a mixed event (convective/stratiform).

This classification enables the analysis of rainfall events composition and the contribution of each precipitation type.

2.3.3. Convective Spells

According to Doswell III [37] and Morin and Yakir [38], there is a very strong correlation between the occurrence of flash floods and the dynamics of convective cells. These cells, which develop within cloud masses, are the source of moderate-to-heavy and sometimes very heavy rainfall, which is known as convective rain. A cloud mass can contain several convective cells, which can evolve at different stages of development. Knowing the duration of convective episodes is therefore important for understanding flash flood generation. Indeed, the time a convective cell stays over a geographical point or a catchment area is related to the amount of rainfall it generates over this area. Consequently, Peleg and Morin [39] linked the life of convective cells to the amount of rain they generated. Belachsen et al. [40] also showed that, in addition to a large area and a lower velocity, the rain cells associated with flash floods are also characterized by the amount of time the convective cell stays over the catchment area.

Based on the above intensity classification, convective episodes in the present study were identified by considering continuous periods (several consecutive time steps) of data during which all intensities are classified as convective. On the other hand, if all intensities in a given period were zero, except for a single intensity with a value above the 10 mm/h threshold, this episode was not classified as a convective episode.

The convective episodes prone to have the greatest hydrological impact (in terms of flooding) are those of a longer duration. Thus, when all the convective episodes of a given rainfall event were identified at a rain gauge, only the longest convective episode was retained, and the associated cumulative rainfall was deduced. These two parameters were then analyzed.

2.3.4. Rainfall Event Parameters

For each identified rainfall event from the average hyetograph representing the global network, the following characteristics were determined:

- The date and time of the beginning of the rainfall event.
- The rainfall event duration.
- The period of the day in which the beginning and the end of the rainfall event are located on the study area: day (06 h–18 h), night (18 h–06 h), or day–night if overlapped.

- The maximum of the maximum intensities in 30 min observed at each of the rain gauges of the network (I_{30max}).

A second group of characteristics was defined on each of the rain gauges:

- The event total rainfall amount at the rain gauge between the beginning and end of a rainfall event defined on the average hyetograph.
- The maximum intensity over a period of 30 min observed at the rain gauge ($I_{30maxpi}$). This parameter is generally used in the evaluation of soil erosivity by rain [41–43]. We considered it rather than maximum rain intensity as a good approximation for the violence of thunderstorms. It can also be used to explain peak flows in the small urban catchments of Abidjan, where the time of concentration is approximately 30 min.
- The duration of the longest convective episode identified with a longer lifetime. This value was determined for each rainfall event and each rain gauge.
- The rainfall amount corresponding to the convective episode identified as having the longest duration.

2.3.5. Other Analyzed Parameters

In addition to the above-mentioned parameters, we extrapolated the number of consecutive days of rainfall events and the probability of occurrence of x and more rainfall events in a single day, with $x \geq 2$.

- Definition of Consecutive Rainy-Day Events (CRDEs):

It is essential to know the number of CRDEs because consecutive days of rainfall provide information on the water amount state of the soil, which can be a factor in increasing runoff and, thus, the risk of flooding [44].

In our study, the fundamental element considered is the rainfall event. In their approach, Wu et al. [45] considered both start and end dates of rainfall events in order to distinguish complete events (start and end in the same day) from partial events (“spread” over two successive days). We used a slightly different approach than Wu et al. [45]. We only considered the start date of the rainfall event to define a rainy-day event. Thus, on this basis, a single rainy-day event is an isolated day that may contain one or more rainfall events, with that day as the starting day. A rainy-day event can contain several rainfall events. Subsequently, two consecutive rainy-day events correspond to two successive days, starting with at least one rainfall event for each of them.

- The probability of exceeding x rainfall events per day.

The probability of occurrence of x or more rainfall events during a single day was defined, based on the date of the beginning of the rainfall events. For each month of the year, we evaluated the number of days with the start of at least two, three, or four rainfall events. This number was then divided by the total number of events for each month, and the resulting probability was analyzed according to the months of the year.

3. Results

3.1. Rainfall Events Identification

A total of 2764 rainfall events were identified from the average hyetograph based solely on an MIT of 30 min and a rain intensity threshold of 0.5 mm/5 min (0.6 mm/h). The duration, rain intensity, and amount (depth) of these events varied. By simultaneously applying the criteria of a minimum duration of 30 min and a minimum rainfall depth of 1 mm, observed in at least one rain gauge, the number of identified rainfall events is reduced by more than half from 2764 to 1240. Figure 3 shows the result of the identification of rainfall events between 7 and 8 November 2021 from the average hyetograph. It is evident that most of the events were identified. The events or time steps not associated with a rainfall event remain marginal in terms of both the quantity and duration of the rain.

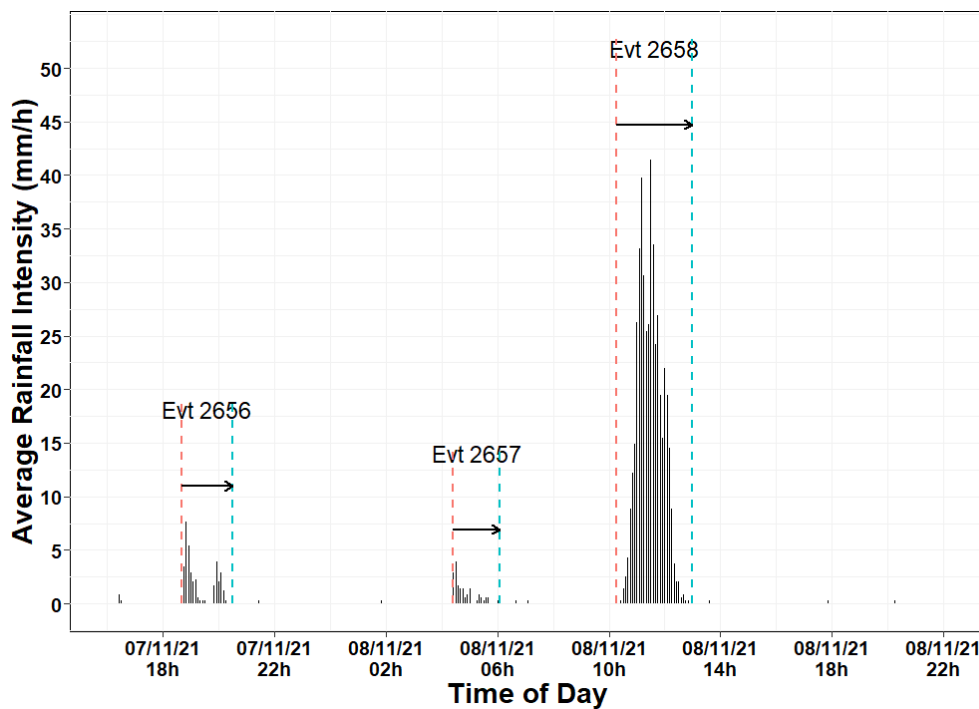


Figure 3. Independent rainfall events where the minimum inter-event time (MIT) is equal to or longer than 30 min, the minimum event duration is 30 min, and at least one rain gauge has a rainfall amount equal to or higher than 1 mm. Each event is delimited by red (start) and green (end) vertical dashed lines. Plotted data are the average rain rates for the area.

Figure 4 below shows event #2658 of Figure 3 above as measured by the rain gauge network. This event was not measured by all the rain gauges as some stations were dysfunctional and some data were missing. The maximum intensity (in 5 min) of this event exceeded 150 mm/h, but this peak of rain rate varied significantly over the network. At the individual rain gauge level, it was obvious that the time of the effective start of the rain, as well as the duration of the rain, was highly variable from one rain gauge to another. However, when working at the network scale, the start time and duration were standardized. The ground signature for the same event can be different depending on the position of the rain gauge in the network. For example, at the rain gauge RIVIERA_NORD_F9, all the intensities exceeded 10 mm/h with several peaks of convective intensities, but at the rain gauge MARCORY, there was only one convective peak.

Over the four years of analyzed data, the 1240 identified rainfall events were distributed as follows in Table 2.

Table 2. The yearly number of rainfall events and rainfall amount.

Year	Network Rainfall Events	Mean Rainfall from Identified Events (mm)	Annual Rainfall from Average Hyetograph (mm)
2018	232	1810	1944
2019	363	1705	1786
2020	293	1884	1943
2021	352	1674	1726
Total	1240		
Interannual average	310	1768	1850

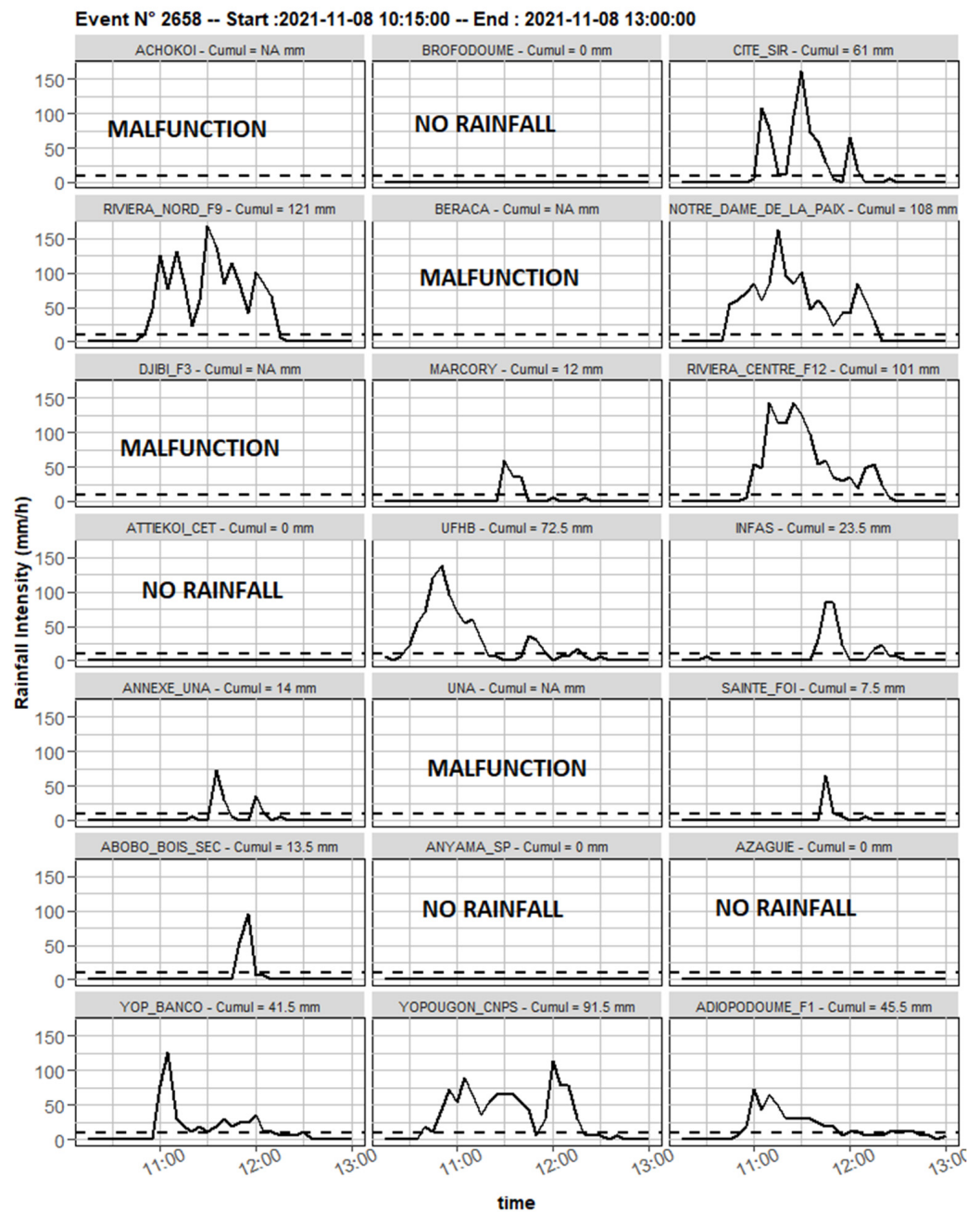


Figure 4. The hyetograph of rainfall event #2658 at each rain gauge of the network. The dashed line indicates the threshold from which the rainfall intensity is considered as convective.

3.2. Rainfall Event Duration

Figure 5 below shows the distribution of the event duration as a function of time. This distribution is related to the rainy seasons, during which the longest rainfall events were observed. From the total event number, events lasting up to 1 h represented 32%, events lasting between 1 h and 2 h represented 33%, and events lasting at least 3 h represented 21.3%. The longest event lasted 1 day 4 h 35 min. The average duration of rainfall events was greater in June (3 h 00 min), followed by July (2 h 50 min), reaching a lower value in January (1 h 17 min) and December (1 h 28) min. Over the study period, the average duration was 2 h 16 min.

3.3. The Rainfall Amount Per Event

Figure 6 below shows the frequency distribution of rainfall events according to their average rainfall amount (including stations that recorded 0 mm of rain). The contribution of each class to annual rainfall amount is also presented as a cumulative curve. It is evident that the average rainfall amount of the identified events over the district of Abidjan, and over the study period, had a distribution dominated by low rainfall amounts with an average of 5.70 mm. The average annual accumulation derived from the average hyetograph is 1768 mm/year (cf. Table 2). More than 85% of rainfall events had an average accumulation not exceeding 10 mm. These 85% produced 32% of the mean annual rainfall. Among the rainfall events producing a significant rainfall, those associated with an average rainfall between 20 mm and 30 mm/event represented 4% and generated 17% of the average annual rainfall. Those associated with an average rainfall exceeding 50 mm/event represented between three and four rainfall events per year for 15% of the average annual rainfall.

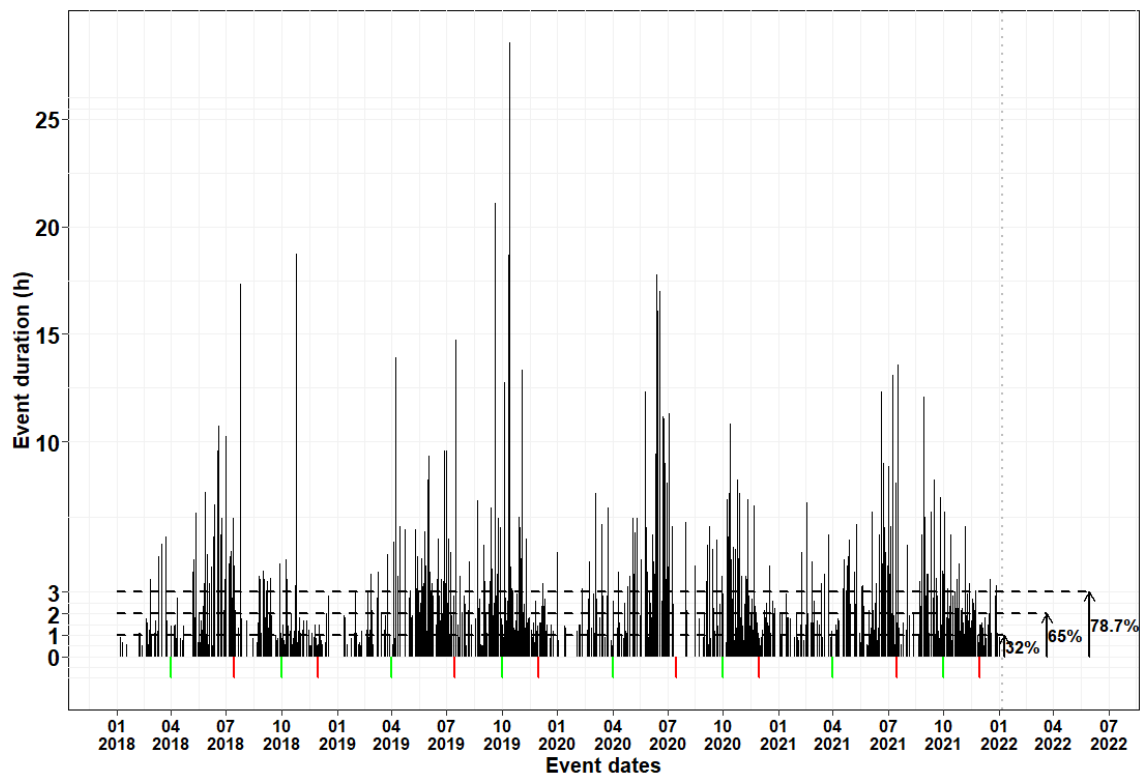


Figure 5. The distribution of rainfall event duration over the study period. The percentages on the right indicate the proportion of events with a duration between 30 min and the arrowhead.

3.4. The Convective/Stratiform Nature of Rainfall Events

In order to analyze the nature of rainfall events, we performed a convective/stratiform classification of intensities at the rain gauges and identified the convective episodes, as shown in Figure 7 for the event of 5 October 2019 observed on the most western rain gauge within the Abidjan District. The convective spells had different durations with variable rain intensities, between 15 min and 4 h 15 min, as well as between 2 mm and 202.5 mm of rainfall. This event was classified as mixed (convective/stratiform) and mainly constituted convective intensities. Within this event and at this rain gauge, the first convective spell was identified as the longest convective spell and associated with a rainfall depth of 202.5 mm.

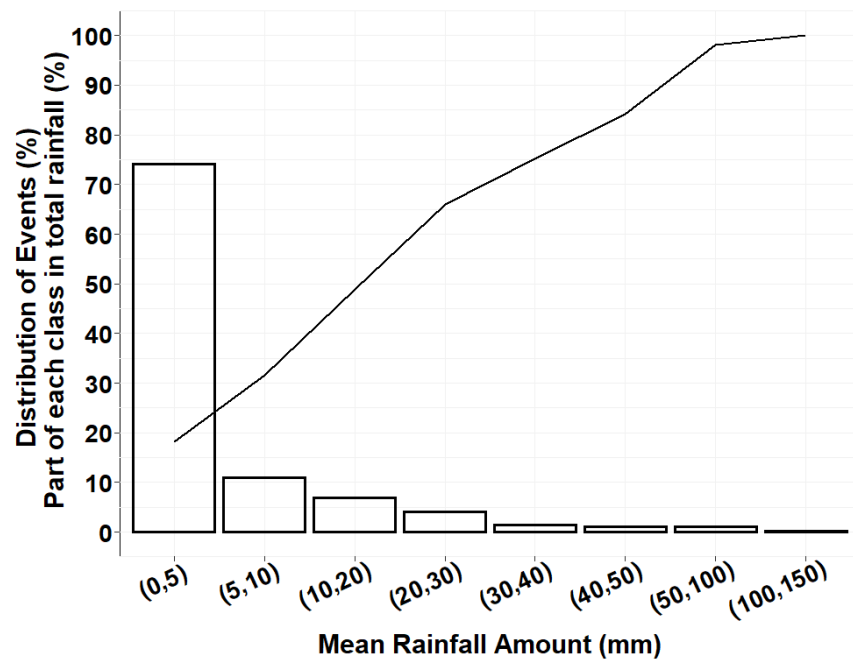


Figure 6. The distribution of the average cumulative rainfall (bar) and the cumulative contribution to the annual rainfall of each class of event average rainfall (line).

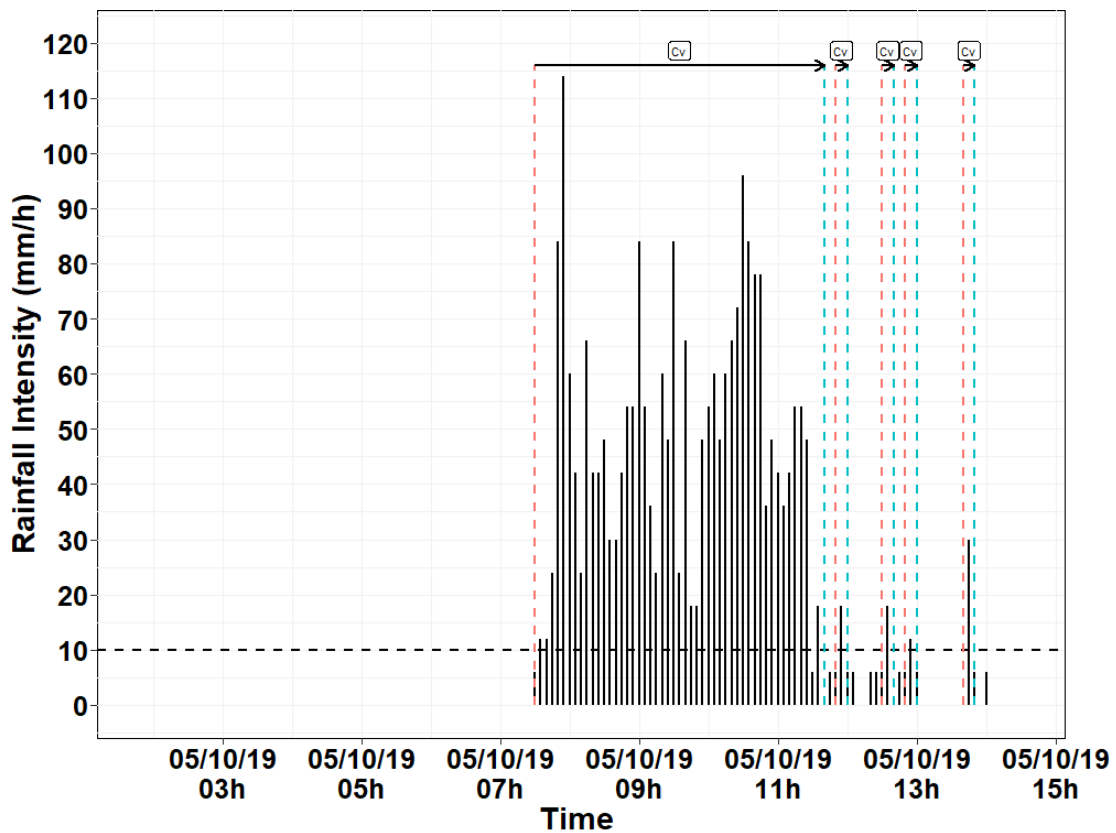


Figure 7. An example of the convective/stratiform classification of intensities and identification of convective episodes for the event of 5 October, 2019 at the Adiopodoumé rain gauge. Horizontal dashes represent the 10 mm/h threshold used for classification. Vertical dashes limit the beginning (red) and end (green) of convective episodes marked by «Cv».

This analysis was carried out for all the events that were identified, and the results are presented in Table 3.

Table 3. The yearly distribution of rainfall events according to their nature.

Year	Convective Events	Stratiform Events	Mixed Events (Convective and Stratiform)
2018	0	47 (20.3%)	185 (79.7%)
2019	0	51 (14.0%)	312 (86.0%)
2020	0	24 (8.2%)	269 (91.8%)
2021	0	30 (8.5%)	322 (91.5%)
Total	0 (0%)	152 (12.3%)	1088 (87.7%)

Over the entire network (100% of rain gauges), no rainfall event was classified as solely convective. However, it should be noted that the majority (87.7%) of rainfall events were the mixed type, compared with only 12.3% of the stratiform type. From year to year, the number of stratiform events did not exceed 20% of the annual number of rainfall events, while for mixed events, this number varied between 80% and 92%.

3.5. Analysis of Convective Spells at the Rain Gauge Scale

For all rainfall events and at each rain gauge, we detected 7083 convective spells. From these, 5116 convective spells were identified as convective episodes with the longest duration in the first convective episode, as seen in Figure 7. These 5116 convective spells of the longest duration at a given rain gauge were distributed, as shown in Figure 8a. The maximum duration of convective spells observed over Abidjan varied between 15 min and 4 h 30 min. However, 4033 (or about 80%) of these long-duration convective spells lasted 45 min or less.

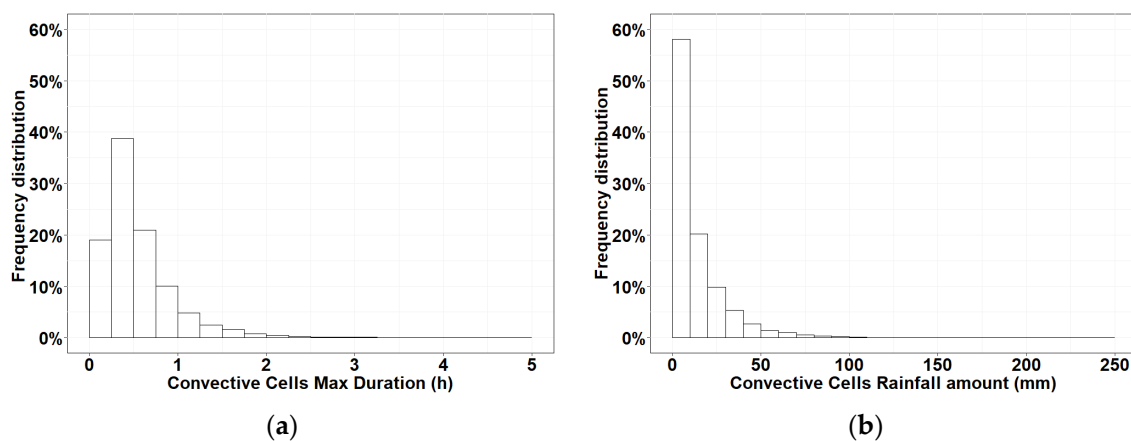


Figure 8. The distribution of the duration of the maximum number of convective episodes within events (a) and the associated cumulative rain (b) observed in the pluviographs for all events.

The rainfall amount generated by each of these maximum duration convective spells is presented in Figure 8b. These rainfall amounts ranged from 2 mm to 203.5 mm, with 2145 (42%) of these convective spells producing a rainfall amount greater than 10 mm, and 830 convective spells (16%) producing at least 25 mm of rainfall.

An analysis of the convective spell duration values by event revealed that the duration of all convective spells for a given rain gauge averaged one quarter (25%) of the total rainfall event duration. For 70% of the mixed rainfall events, the convective spells lasted up to 33.33% of the total event duration, and they produced an average of 80% of the cumulative event at the rain gauge.

3.6. The Most Intense Rainfall Intensity: I30max

The average maximum rain intensity in 30 min (I30max, cf. Figure 9) was related to its time of occurrence, relative to the duration of the event, i.e., as a percentage of the total duration of the rainfall event.

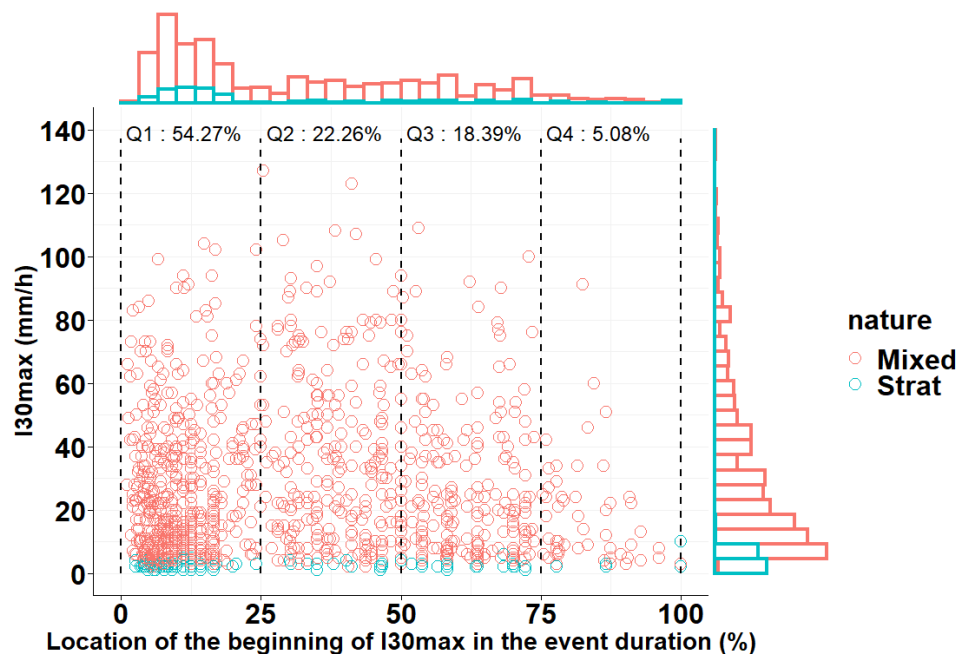


Figure 9. The I30max as a function of their location in storm duration and distribution of the I30max and their time of occurrence. Each open circle represents one event. Salmon pink dots are events classified as mixed (convective and stratiform) and teal dots represent stratiform events.

The results indicate that an I30max can occur at any time during the duration of a rainfall event. However, more than half of the events (54%) see their I30max in the first quarter (25%) of their duration, and 76% see it in the first half of the event. Only 5% of the events had their peak of intensity in the last quarter of the total event duration.

Events generally classified as stratiform were associated with the lowest I30max values. For most of these events, the I30max also occurred in the first quarter of the total duration of the rainfall event.

Over 30 min, the maximum intensity reached very high values with a maximum at 127 mm/h, and 13.5% (i.e., 168) of the events had an I30max higher than 50 mm/h.

The proportion of rainfall during the 30 wettest minutes compared to the event total rainfall amount at the rain gauge is presented in Figure 10. For more than 80% of the events, the most intense 30 min brought more than 50% of the event rainfall at the rain gauge.

In general, in more than 75% of cases, these events had their peak intensity over a 30-min period in the first half of the total duration of the event. On average, the I30max brought more than 75% of the cumulative event to the rain gauge.

3.7. The Diurnal Cycle

- Rainfall event starting time

The starting times of the rainfall events were grouped into 3 h periods. The results are presented, as distribution, in Figure 11. This figure shows that a rainfall event could start at any time of the day. However, some time periods appear as preferential moments, following the diurnal cycle of sunshine. Indeed, the highest occurrence (~24%) was observed between 12 pm and 3 pm, and more than half of the events (54%) started between 9 am and 6 pm. The different times during the night showed similar occurrences. There was no preferred time for the start of the stratiform rainfall.

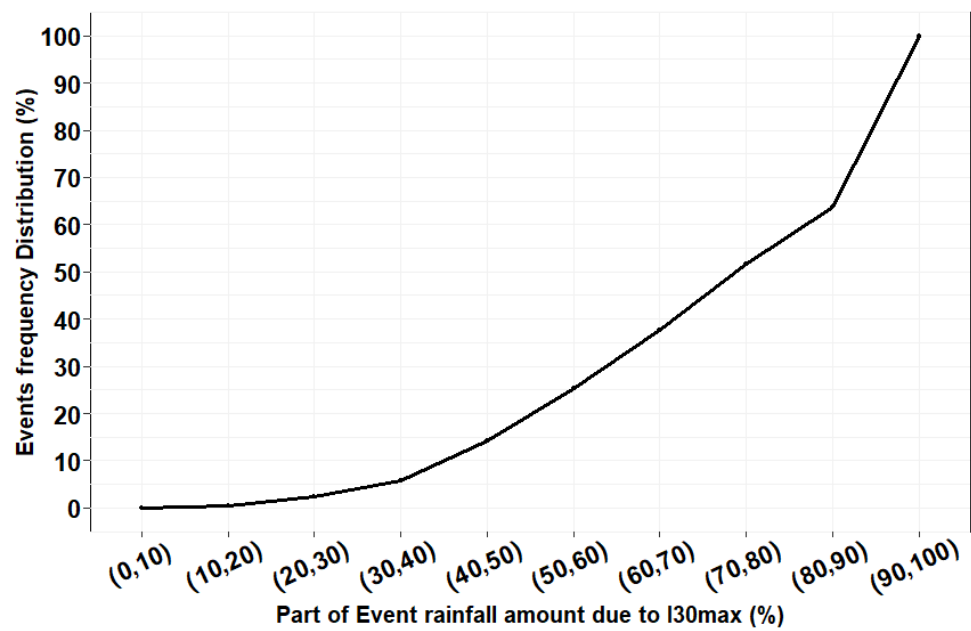


Figure 10. The distribution of the proportion of event rainfall due to the I30max at the associated rain gauge for all events.

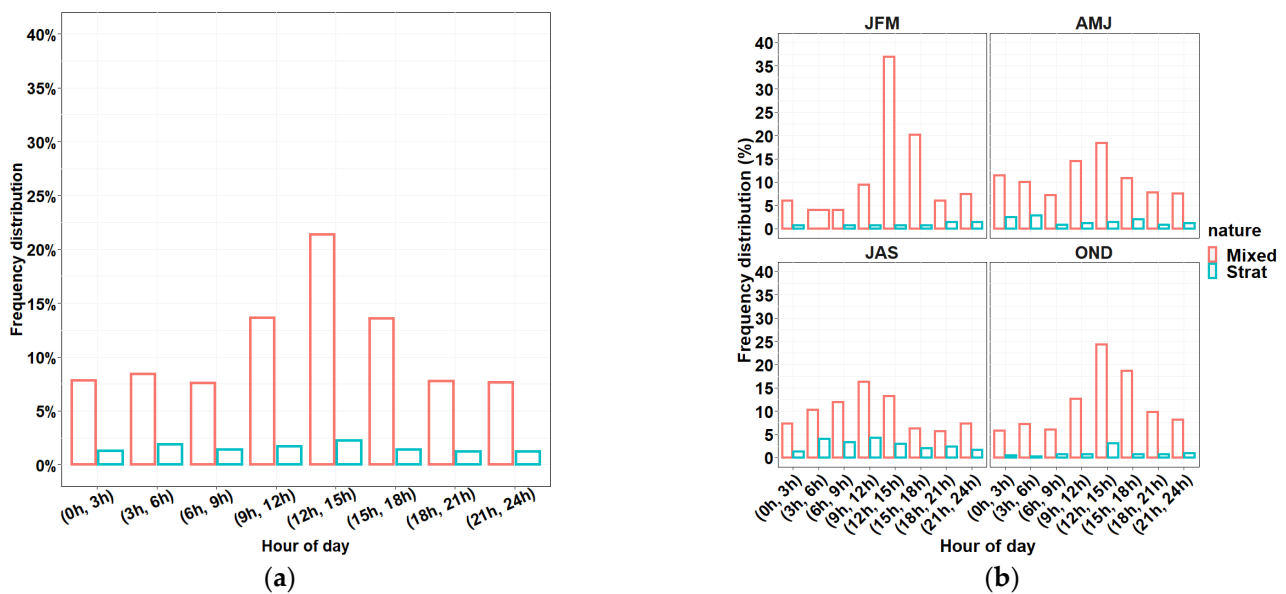


Figure 11. The distribution of the rainfall event starting time. Grey bars represent stratiform events, while white bars represent mixed (convective and stratiform) events: (a) The distribution is presented for whole period independently to the season; (b) The distribution is presented quarterly: JFM stands for January–February–March, AMJ for April–May–June, JAS for July–August–September, and OND for October–November–December.

The quarterly analysis shows some differences. We noted a double peak in April–May–June (AMJ), with the minor peak in the middle of the night and the major peak during the day as with the other quarters. We also observed that July–August–September (JAS) is the quarter with the highest probability of stratiform events compared to mixed events. In October–November–December (OND), they tended to appear in the middle of the day, while in AMJ, it was in the middle of the night that we noted a significant probability of appearance.

- Position of the rainy period during the day

More than half of the rainy events (56.2%) started and ended during the day between 6 am and 6 pm, compared to 28.6% between 6 pm and 6 am (overnight) as shown in Table 4. The events crossing these two periods represent about 15.2%. For every two daytime events, one nighttime event is recorded. Whatever the time of day, mixed events predominated.

Table 4. The percentage of events relative to their nature and their starting and ending time. The numbers of events are indicated in brackets.

Moment of Day	Nature of Event	Percentage (Number of Event)	Total
Day	Mixed (Convective and Stratiform)	50.1% (621)	56.2% (697)
	Stratiform	06.1% (76)	
Night	Mixed (Convective and Stratiform)	23.6% (293)	28.6% (355)
	Stratiform	05.0% (62)	
Day–Night	Mixed (Convective and Stratiform)	14.0% (174)	15.2% (188)
	Stratiform	01.1% (14)	
Total	Mixed (Convective and Stratiform)	87.7% (1088)	100% (1240)
	Stratiform	12.3% (152)	

3.8. Rainfall Event Occurrence

The 1240 rainfall events occurred over 732 days, an average of 1.58 rainfall events per rain day, while 58% of the rainy days were due to a single rainfall event. These results are presented in Table 5 below. The maximum number of events observed during a single day was seven.

Table 5. Daily occurrence of rainfall events.

Number of Events Per Day	1	2	3	4	5	6	7
Occurrence (percentage)	424 (57.9%)	184 (25.1%)	73 (10.0%)	33 (4.5%)	12 (1.6%)	5 (0.7%)	1 (0.1%)

An analysis of the probabilities of exceeding two, three, or four events in a single day by month of the year is shown in Figure 12. The probabilities were highest between June and November. The highest probabilities of two, three, or four events per day were observed during the months of June and October, corresponding to the core of the rainy seasons. While the probability of having at least two events/day exists and was significant throughout the year, during January and February, no day recorded three or more events. From March onwards, the probability of four or more events per day became non-zero.

3.9. Consecutive Rainy-Day Events (CRDEs)

The distribution of consecutive rainy-day events (successive days with rainfall events) is presented in Figure 13. Over the study period, isolated rainy days represented 125 days out of the 732 rainy days counted, i.e., 17.2%. These isolated rainy days were more frequent outside the rainy-season months.

The duration of the CRDEs ranged from 2 to 22 consecutive days. The most frequent durations of CRDEs were 2, 3, 4, 5, and 6 days, with the entire range from 8 to 57 days. The highest occurrence (57) was obtained with 2 consecutive days of rainfall events. The longest duration (22 days) of consecutive days of rainfall events corresponds to the period from 5 to 26 November 2020.

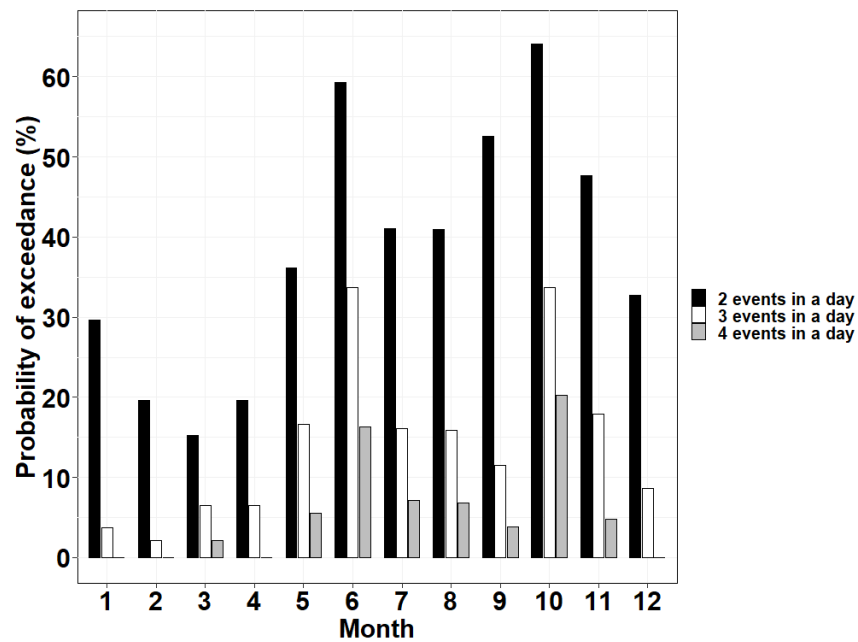


Figure 12. The probability of observing at least two, three, or four events per day in a given month.

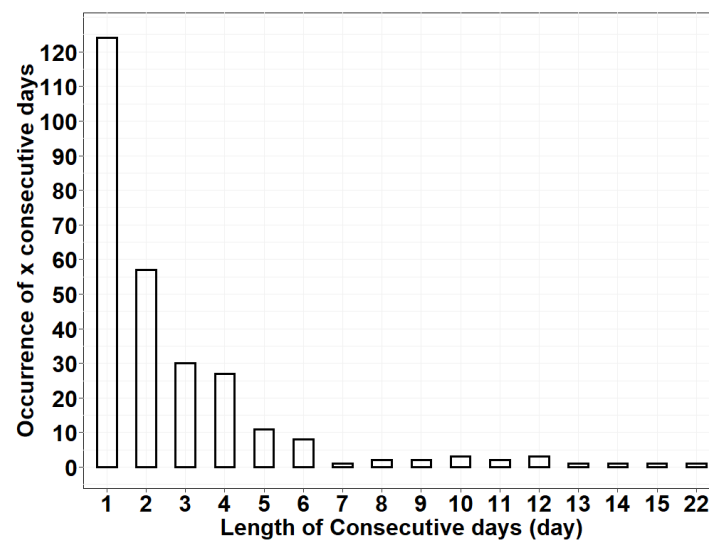


Figure 13. Distribution of consecutive rainy-day events. The first value (1) represents the isolated days of rainfall events.

4. Discussion

In this study, by combining the minimum inter-event time without a rainfall of 30 min, a minimum average rainfall accumulation threshold of 0.05 mm in our study area. With the minimum duration of 30 min and the minimum accumulation observed at a rain gauge, we isolated 1240 individual rainfall events in the Abidjan District. This represents an average of 310 rainfall events per year associated with 183 rainy days.

Our criteria for identifying rainfall events are similar to those used by D’Amato and Lebel [30] in Niger (Niamey square degree) in the Sahelian zone and Zahiri et al. [46] in Northern Benin in the Sudanian zone (Upper Ouémé Valley). However, in their approach, these authors considered that an event was valid if at least 30% of the rain gauges in the network recorded at least 1 mm of rain each. Such a criterion can lead to the exclusion of rainfall events detected at the edge of the network. Furthermore, in some previous studies, the definition of a rainfall event was based on data from a single rain gauge [21,47,48].

This shows that even without applying a minimum percentage of affected rain gauges, the network aspect is well-considered at the beginning of our analysis. This network approach, accounting equally for the beginning and the duration of the rainfall event over our study area, effectively accounts for the variability of rainfall during the same rainfall event. This variability can lead to different shapes of the hyetograph at each point of the network. By analyzing rainfall events from multiple rain gauges within a network, we can obtain more information for a better characterization of rainfall. The progressive deployment of rain gauges in the network had a little impact on the number of rainfall events detected. Indeed, in 2020, when we had more rain gauges than in 2019, 20% fewer rainfall events were detected. As suggested by Dunkerley, it is the minimum inter-event time that has the most important influence on the number and duration of rainfall events. The choice of a 30 min MIT seems appropriate for the scale of the network. It should be noted that at the level of the rain gauges, there may remain minimum inter-event times greater than 30 min (see Figure 7). A longer minimum inter-event time would result in many cases of merging distinct events into one. In a study using a single rain gauge located at Adiopodoumé (in Abidjan), researchers Sighomnou and Desbordes [49] considered a minimum inter-event time of 6 h from a hydrological perspective to ensure that the hydrographs of two successive events would be totally independent. In addition, to focus on events with a significant hydrological impact, they considered a threshold accumulation of 25 mm in 24 h. They were thus able to identify 190 rainfall events over a period of 16 years of data (i.e., 12 events/year). On the station with the most complete series over the period 2018–2021, we were able to identify 84 rainfall events with a cumulative event at least equal to 25 mm (or 21 events/year). For our network's rain gauge, also located in Adiopodoumé, 52 rainfall events of the same type were identified over a period of 3 years (i.e., 17 events/year). These differences observed in terms of the average number of events, which can be up to double for the recent period, can be explained firstly by the criteria for defining rainfall events with a 6 h MIT on the rain gauge, as opposed to a 30 min MIT at the network level in our study. The decrease in the number of events for increasingly larger MITs was precisely noted by Dunkerley [14]. Secondly, the study period in Sighomnou and Desbordes [49] included the major droughts that hit the region in the 1970s and 1980s [50]. Yao et al. [51] showed a decrease in the number of rainy days and daily extremes between 1970 and 1990.

Over the Niamey square degree (16,000 km²), D'Amato and Lebel [30] identified 223 events between 1990 and 1994 as part of the EPSAT–Niger experiment with an average of 43 events per year. In the same area, with a longer series (1990–2002) and still using the criteria of D'Amato and Lebel [30], Balme-Debionne [52] identified 548 rainfall events, i.e., an average of 42 events per year. In northern Benin, in the Upper Ouémé Valley watershed with a surface area of 14 600 km², Lawin [53] found an annual average of 105 events per year over an analysis period of 7 years (1999–2005) using the same criteria as Niamey. In comparison to these different studies, the average annual number of rainfall events observed in the Abidjan District (coastal zone) is three times higher than that obtained in Northern Benin (Sudanian zone) and seven times higher than that observed in Niamey (Sahelian zone). This variation in the number of rainfall events is consistent with the rainfall gradient over West Africa, with the highest cumulative rainfall observed along the West African coast. Indeed, over the West African region, the cumulative rainfall decreases when moving away from the coast. However, if we consider the non-zero cumulative rainfall, we observe a major difference in rainfall per event, which averages 11.30 mm per event in Abidjan, 12.1 mm in North Benin, and 13 mm in Niger, according to Lawin [53]. The proximity of the Abidjan District to the ocean certainly contributes significantly to the generation of rainfall events because the ocean is the reservoir of atmospheric moisture, as shown by Amouin et al. [54].

Over Abidjan, the events in the present study were mostly (87%) identified as mixed (convective and stratiform). According to Houze [55], stratiform rainfall is directly related to deep convection. It is the dying convective cells that feed the stratiform part of the convective system [56]. We can therefore affirm that the rainfall events observed over

Abidjan are of convective origin. This conclusion agrees with previous studies on the region, which have shown that in the West African sub-region, rainfall events are mainly from convective origin: Depraetere et al. [57] over Northern Benin, Mathon et al. [5] over the Sahel, and Maranan [58] over the southern part of West Africa.

In terms of duration, the events identified in the Abidjan District, with an average duration of 2 h 16 min, have shorter duration than those identified at sites far from the coastal area. In North Benin, Lawin [53] found an average duration per event of about 5 h. In his PhD thesis, Mathon [6] showed that the convective systems south of 9° N are less organized and, over the Côte d'Ivoire, these systems also have short lifetimes. Maranan et al. [59] and Camberlin et al. [60] also noted these characteristics of less-organized, smaller, and more short-lived systems along the West African coast. However, beyond meteorological considerations, the difference in the size of the three rain gauge networks could also partly explain the differences observed in the duration of rainfall events. Indeed, the area of the Abidjan District is 6.8 and 7.5 times smaller than that of Benin and Niger, respectively.

In the Abidjan District, more than half of the rainiest 30 min begin in the first quarter of the event's duration. For Sighomnou and Desbordes [49], the period of maximum intensity in 30 min is even closer to the beginning of the event: they found that 60% of the events see their peak intensity between 0 and 10% of the event duration. However, they were very selective in defining the rainfall events, which were studied at a more local scale (at the rain gauge), whereas we worked at the network scale, which influenced the duration of the rainfall event. Thus, the position of I30max was incorporated. Nel et al. [61] indicated the importance of the position of the intensity peak, as well as the major role of the intensity of I30max on infiltration, runoff, and erosion. In Mauritius, its research showed that peak intensities occurring at the beginning of the event (the first half of the total duration) lead to less runoff and soil erosion than the peaks at the end of the event. This observation seems to be in contrast to what is seen in our region where the most violent convective systems, sometimes the cause of disasters, are squall lines as judged by Gaye et al. [62]. These systems bring the most intense precipitation within the convective part at the beginning of the event after a wind squall [55,62]. Identified convective spells of maximum duration are short—equivalent to less than one-third of the duration of the event—but bring the important part of the event rainfall (an average of 80%). For flood impacts reduction, convective spells need to be monitored. In fact, as shown by Sangiorgio and Barindelli [63], long-lasting convective cells present a higher probability of generating hydrometeorological risks. Events containing such convective spells produced very important rainfall. Extreme rainfall events producing rainfall greater than 50 mm/event are rare, just over 1%, but they are certainly associated with some flood events in the Abidjan District. In fact, they bring 15% of the mean annual rainfall.

The evolution of the diurnal cycle of rainfall during our study period shows that over the District of Abidjan, it can rain at any time of the day. However, the most favorable period during the day is between 9 am and 6 pm with a peak between 12 pm and 3 pm that corresponds to the time of day when convection reaches its peak of activity along the coast of the Gulf of Guinea. This peak appears much earlier than far from the coast as shown by Janiga and Thorncroft [64]. Inland, away from the West African coast, the convective peak generally appears in the 3 pm–6 pm range. According to Maranan et al. [59], on the West African coast, land–ocean interactions favor the development of intense local convection through the convergence of the sea breeze. In April–May–June (AMJ), there is a nocturnal peak between 0 am and 3 am at the start of the events. According to Zhang et al. [65], these nocturnal rains, also observed in the diurnal cycle of cumulative rainfall and average intensities, can be attributed to propagative convective systems initiated at least in the afternoon of the previous day further east, thus outside the borders of Côte d'Ivoire.

During the active phases of the monsoon, the particular atmospheric conditions that are established over the region are called key characteristics of the West African monsoon [66]. These characteristics include, among others, the formation of the African Easterly Jet (AEJ, 600–700 hPa) inducing the development of easterly waves that strongly

interact with convection and are favorable to the development of convective systems that cause heavy rainfall. This is potentially why the probability of observing several events per day and on several consecutive days is higher between June and November, with a peak in June and October. These months during which the West African monsoon is active on the coast correspond to the coastal phase from April to June according to Thornicroft et al. [67], and to the phase of retreat towards the south, which takes place from September to October [68]. This retreat phase corresponds to the installation of the second rainy season on the coast, which lasts until November. Between July and August, the relatively high number of days with more than two rainfall events is mainly due to the warm rains observed during this period [59], which explains the high proportion of stratiform events (Figure 10b—July–August–September (JAS)).

5. Conclusions

This study presents an analysis of the characteristics of rainfall events over the equatorial zone bordering the Gulf of Guinea. In order to study urban flooding, a network of 21 rain gauges was progressively deployed since 2015 in the Abidjan District. A better knowledge of individual rainfall events is essential in order to find solutions to reduce the effects of hydrometeorological risks. Over the 2018–2021 period, we identified 1240 individual rainfall events in the EVIDENCE project rain gauge network. This corresponds to an inter-annual average of 310 rainfall events. These events lasted on average more than two hours with a rainfall of 11.30 mm/event. The peak rainfall was observed between 12 pm and 3 pm, when the convection is also at its peak of activity. The rainfall events observed over Abidjan were essentially of convective origin with 20% classified as “purely” stratiform compared to 80% classified as mixed events, i.e., convective/stratiform. For 70% of the mixed rainfall events, the convective episodes lasted up to 33.33% of the total duration of the event and yielded an average of 80% of the cumulative rainfall. For 3/4 of all identified events and 3/4 of the events with an I30max exceeding 50 mm/h, the rainiest 30 min (I30max) occurred essentially during the first half of the duration of the rainfall event. The I30max represents on average more than 3/4 of the cumulative rainfall at the rain gauge. In the middle of the two rainy seasons, there was a high probability of having more than two events per day, which increases the risk of flooding in case of a succession of intense rainfall events. During these rainy periods, although the individual events should be monitored from start to finish, particular attention should be focused on the first half of the rainfall event duration.

Detailed information based on each individual rainfall event is, thus, available. This opens the door to further studies on the identification and analysis of rainfall events responsible for flooding in the Abidjan District and the study of their hydrological impact. Notably, these analyses can be undertaken at the level of the rain gauge and some parameters, such as the effective duration of rainfall at the rain gauge, can be estimated for each event.

Author Contributions: Conceptualization, M.K. and E.-P.Z.; Methodology, M.K.; Software, M.K. and K.C.Y.; Validation, E.-P.Z., K.C.Y., L.S., C.D., E.S.K., J.-L.P., A.D., A.A.F.K., K.F.K. and K.T.T.; formal analysis, M.K., E.-P.Z. and L.S.; Investigation, C.D., E.S.K., J.-L.P., A.D., A.A.F.K., K.F.K. and K.T.T.; Data curation, C.D., E.S.K., J.-L.P., A.D., A.A.F.K., K.F.K. and K.T.T.; Writing—original draft preparation, M.K.; Writing—review and editing, E.-P.Z., K.C.Y., L.S., C.D., E.S.K., J.-L.P., A.D., A.A.F.K., K.F.K. and K.T.T.; Visualization, M.K., E.-P.Z., K.C.Y., L.S., C.D., E.S.K., J.-L.P., A.D., A.A.F.K., K.F.K. and K.T.T.; Project administration, E.-P.Z. and M.K.; Funding acquisition, E.-P.Z., M.K., L.S. and J.-L.P. All authors have read and agreed to the published version of the manuscript.

Funding: The project leading to this work has received funding from the “Partenariat rénové pour la Recherche au Service du Développement de la Côte d’Ivoire” under the grant number PRESED-CI-C2D-Projet EVIDENCE 305984/00/5768A1-PEV. We acknowledge the EVIDENCE Project for providing the dataset used in the framework of this research.

Institutional Review Board Statement: Not applicable.

Informed Consent Statement: Not applicable.

Data Availability Statement: Data available from the corresponding author upon request.

Acknowledgments: We acknowledge the EVIDENCE Project for providing the dataset used in the framework of this research.

Conflicts of Interest: The authors declare no conflict of interest.

References

1. Boberg, J. Freshwater Availability. In *Liquid Assets; How Demographic Changes and Water Management Policies Affect Freshwater Resources*; RAND Corporation: Santa Monica, CA, USA, 2005; pp. 15–28; ISBN 978-0-8330-3296-6.
2. Sy, A.; Durooure, C.; Baray, J.-L.; Gour, Y.; Van Baelen, J.; Diop, B. Space-Time Variability of the Rainfall over Sahel: Observation of a Latitudinal Sharp Transition of the Statistical Properties. *Atmosphere* **2018**, *9*, 482. [CrossRef]
3. Tarhule, A. Damaging Rainfall and Flooding: The Other Sahel Hazards. *Clim. Change* **2005**, *72*, 355–377. [CrossRef]
4. Nouaceur, Z. La reprise des pluies et la recrudescence des inondations en Afrique de l’Ouest sahélienne. *Physio-Géo. Géographie Phys. Environ.* **2020**, *15*, 89–109. [CrossRef]
5. Mathon, V.; Laurent, H.; Lebel, T. Mesoscale Convective System Rainfall in the Sahel. *J. Appl. Meteorol.* **2002**, *41*, 1081–1092. [CrossRef]
6. Mathon, V. Etude Climatologique des Systemes Convectifs de Meso-Echelle en Afrique de l’ouest, Mathon, Vincent. Ph.D. Thesis, Université Paris 7—Denis Diderot, Paris, France, 2001.
7. OCHA Côte d’Ivoire. Zones à risques d’inondations et de choléra. *Portail sur la résilience aux inondations*. 2014. Available online: <https://resilience-inondations.net/ressources/item/cote-divoire-zones-a-risques-dinondations-et-de-cholera/> (accessed on 30 June 2022).
8. Traoré, H.K. Appréhender L’urbanisation en Milieu Tropical Humide: Le cas du Grand Abidjan. Le 4 Pages du LOTERR n°10, Décembre 2021. 2021. Available online: <https://hal.univ-lorraine.fr/hal-03472004> (accessed on 15 February 2023).
9. Kangah, A.; Della, A.A. Détermination des zones à risque d’inondation à partir du modèle numérique de terrain (MNT) et du système d’information géographique (SIG): Cas du bassin-versant de Bonoumin-Palmeraie (commune de Cocody, Côte d’Ivoire). *Geo-Eco-Trop* **2015**, *39*, 297–308.
10. Peters, O.; Christensen, K. Rain Viewed as Relaxational Events. *J. Hydrol.* **2006**, *328*, 46–55. [CrossRef]
11. Wang, W.; Yin, S.; Xie, Y.; Nearing, M.A.; Wang, W.; Yin, S.; Xie, Y.; Nearing, M.A. Minimum Inter-Event Times for Rainfall in the Eastern Monsoon Region of China. *Trans. ASABE* **2019**, *62*, 9–18. [CrossRef]
12. Yen, B.C.; Chow, V.T. *Local Design Storm: Volume 2. Methodology and Analysis, FHWA-RD-82-064*; United States. Federal Highway Administration. Offices of Research and Development: Washington, DC, USA, 1983. Available online: <https://rosap.ntl.bts.gov/view/dot/41863> (accessed on 20 December 2021).
13. Svoboda, V.; Hanel, M.; Máca, P.; Kyselý, J. Characteristics of Rainfall Events in Regional Climate Model Simulations for the Czech Republic. *Hydrol. Earth Syst. Sci.* **2017**, *21*, 963–980. [CrossRef]
14. Dunkerley, D. Identifying Individual Rain Events from Pluviograph Records: A Review with Analysis of Data from an Australian Dryland Site. *Hydrol. Process.* **2008**, *22*, 5024–5036. [CrossRef]
15. Wang, F. Temporal Pattern Analysis of Local Rainstorm Events in China During the Flood Season Based on Time Series Clustering. *Water* **2020**, *12*, 725. [CrossRef]
16. Sottile, G.; Francipane, A.; Adelfio, G.; Noto, L.V. A PCA-Based Clustering Algorithm for the Identification of Stratiform and Convective Precipitation at the Event Scale: An Application to the Sub-Hourly Precipitation of Sicily, Italy. *Stoch. Environ. Res. Risk Assess.* **2021**, *36*, 2303–2317. [CrossRef]
17. Terranova, O.G.; Gariano, S.L. Rainstorms Able to Induce Flash Floods in a Mediterranean-Climate Region (Calabria, Southern Italy). *Nat. Hazards Earth Syst. Sci.* **2014**, *14*, 2423–2434. [CrossRef]
18. Joo, J.; Lee, J.; Kim, J.H.; Jun, H.; Jo, D. Inter-Event Time Definition Setting Procedure for Urban Drainage Systems. *Water* **2014**, *6*, 45–58. [CrossRef]
19. Nojumuddin, N.S.; Yusof, F.; Yusop, Z. Determination of Minimum Inter-Event Time for Storm Characterisation in Johor, Malaysia. *J. Flood Risk Manag.* **2018**, *11*, S687–S699. [CrossRef]
20. Ignaccolo, M.; De Michele, C. A Point Based Eulerian Definition of Rain Event Based on Statistical Properties of Inter Drop Time Intervals: An Application to Chilbolton Data. *Adv. Water Resour.* **2010**, *33*, 933–941. [CrossRef]
21. Barbosa, L.R.; de Oliveira Galvão, C.; de Araújo, J.C. Sub-Hourly Rainfall Patterns by Hyetograph Type under Distinct Climate Conditions in Northeast of Brazil: A Comparative Inference of Their Key Properties. *Rbrh* **2018**, *23*, 14. [CrossRef]
22. Larsen, M.L.; Teves, J.B. Identifying Individual Rain Events with a Dense Disdrometer Network. *Adv. Meteorol.* **2015**, *2015*, 1–12. [CrossRef]
23. Dunkerley, D. How Is the Intensity of Rainfall Events Best Characterised? A Brief Critical Review and Proposed New Rainfall Intensity Index for Application in the Study of Landsurface Processes. *Water* **2020**, *12*, 929. [CrossRef]
24. Löwe, R.; Madsen, H.; McSharry, P. Objective Classification of Rainfall in Northern Europe for Online Operation of Urban Water Systems Based on Clustering Techniques. *Water* **2016**, *8*, 87. [CrossRef]
25. He, S.; Wang, J.; Liu, S. Rainfall Event–Duration Thresholds for Landslide Occurrences in China. *Water* **2020**, *12*, 494. [CrossRef]

26. Sodexam Saison des Pluies 2020: LES Precisions du Directeur de la Meteorologie Nationale—2020. Available online: http://www.sodexam.com/?page_id=4089 (accessed on 20 May 2022).
27. Zahiri, E.; Séguis, L.; Kacou, M.; Kamagaté, B.; Dao, A.; Perrin, J.-L.; Koffi, S.E.; Guilliod, M. 5 minutes rainfall in Abidjan district (Côte d’Ivoire) (2015-). *Datasuds* **2022**, *5*. [[CrossRef](#)]
28. Ochou, A.D.; Kouadio, K.; Marchant, J.; Yapo, C.; Sauvageot, H.; Achy, S.A. Etude des précipitations par satellite en Côte d’Ivoire. *Veill. Clim. Satellitaire* **1991**, *38*, 57–62.
29. Kouamé, B. *Forme des Averses Variabilité Spatiale et Temporelle au Nord Ouest de la Cote O-Ivoire*; Université des Sciences et Techniques du Languedoc: Languedoc-Roussillon, France, 1987; p. 141.
30. D’Amato, N.; Lebel, T. On the Characteristics of the Rainfall Events in the Sahel with a View to the Analysis of Climatic Variability. *Int. J. Climatol.* **1998**, *18*, 955–974. [[CrossRef](#)]
31. Duque, L.F. IETD: Inter-Event Time Definition. R Package Version 1.0.0. 2020. Available online: <https://CRAN.R-project.org/package=IETD> (accessed on 21 February 2021).
32. R Core Team. *R: A Language and Environment for Statistical Computing*; R Foundation for Statistical Computing: Vienna, Austria, 2019.
33. Testud, J.; Oury, S.; Black, R.A.; Amayenc, P.; Dou, X. The Concept of “Normalized” Distribution to Describe Raindrop Spectra: A Tool for Cloud Physics and Cloud Remote Sensing. *J. Appl. Meteorol. Climatol.* **2001**, *40*, 1118–1140. [[CrossRef](#)]
34. Moumouni, S.; Gosset, M.; Houngninou, E. Main Features of Rain Drop Size Distributions Observed in Benin, West Africa, with Optical Disdrometers. *Geophys. Res. Lett.* **2008**, *35*, L23807. [[CrossRef](#)]
35. Zeng, Y.; Yang, L.; Zhang, Z.; Tong, Z.; Li, J.; Liu, F.; Zhang, J.; Jiang, Y. Characteristics of Clouds and Raindrop Size Distribution in Xinjiang, Using Cloud Radar Datasets and a Disdrometer. *Atmosphere* **2020**, *11*, 1382. [[CrossRef](#)]
36. Wu, Z.; Zhang, Y.; Zhang, L.; Zheng, H.; Huang, X. A Comparison of Convective and Stratiform Precipitation Microphysics of the Record-Breaking Typhoon In-Fa (2021). *Remote Sens.* **2022**, *14*, 344. [[CrossRef](#)]
37. Doswell III, C.A.; Brooks, H.E.; Maddox, R.A. Flash Flood Forecasting: An Ingredients-Based Methodology. *Weather Forecast.* **1996**, *11*, 560–581. [[CrossRef](#)]
38. Morin, E.; Yakir, H. Hydrological Impact and Potential Flooding of Convective Rain Cells in a Semi-Arid Environment. *Hydrol. Sci. J.* **2014**, *59*, 1353–1362. [[CrossRef](#)]
39. Peleg, N.; Morin, E. Convective Rain Cells: Radar-Derived Spatiotemporal Characteristics and Synoptic Patterns over the Eastern Mediterranean. *J. Geophys. Res. Atmos.* **2012**, *117*, D15116. [[CrossRef](#)]
40. Belachsen, I.; Marra, F.; Peleg, N.; Morin, E. Convective Rainfall in a Dry Climate: Relations with Synoptic Systems and Flash-Flood Generation in the Dead Sea Region. *Hydrol. Earth Syst. Sci.* **2017**, *21*, 5165–5180. [[CrossRef](#)]
41. de Lima, C.A.; de Palácio, H.A.Q.; de Andrade, H.A.Q.; dosSantos, J.C.N.; Brasil, P.P. Characteristics of Rainfall and Erosion under Natural Conditions of Land Use in Semiarid Regions. *Rev. Bras. Eng. Agríc. Ambient.* **2013**, *17*, 1222–1229. [[CrossRef](#)]
42. Lee, J.; Lee, S.; Hong, J.; Lee, D.; Bae, J.H.; Yang, J.E.; Kim, J.; Lim, K.J. Evaluation of Rainfall Erosivity Factor Estimation Using Machine and Deep Learning Models. *Water* **2021**, *13*, 382. [[CrossRef](#)]
43. Wu, L.; Liu, X.; Ma, X. Spatiotemporal Distribution of Rainfall Erosivity in the Yanhe River Watershed of Hilly and Gully Region, Chinese Loess Plateau. *Environ. Earth Sci.* **2016**, *75*, 315. [[CrossRef](#)]
44. Zheng, Y.; Li, S.; Ullah, K. Increased Occurrence and Intensity of Consecutive Rainfall Events in the China’s Three Gorges Reservoir Area Under Global Warming. *Earth Space Sci.* **2020**, *7*, e2020EA001188. [[CrossRef](#)]
45. Wu, S.-J.; Tung, Y.-K.; Yang, J.-C. Incorporating Daily Rainfall to Derive At-Site Hourly Depth-Duration-Frequency Relationships. *J. Hydrol. Eng.* **2009**, *14*, 992–1001. [[CrossRef](#)]
46. Zahiri, E.-P.; Bamba, I.; Famién, A.M.; Koffi, A.K.; Ochou, A.D. Mesoscale Extreme Rainfall Events in West Africa: The Cases of Niamey (Niger) and the Upper Ouémé Valley (Benin). *Weather Clim. Extrem.* **2016**, *13*, 15–34. [[CrossRef](#)]
47. Dunkerley, D. Intra-Event Intermittency of Rainfall: An Analysis of the Metrics of Rain and No-Rain Periods. *Hydrol. Process.* **2015**, *29*, 3294–3305. [[CrossRef](#)]
48. Dunkerley, D.L. Rainfall Intensity Bursts and the Erosion of Soils: An Analysis Highlighting the Need for High Temporal Resolution Rainfall Data for Research under Current and Future Climates. *Earth Surf. Dyn.* **2019**, *7*, 345–360. [[CrossRef](#)]
49. Sighomnou, D.; Desbordes, M. Recherche d’un modèle de pluie de projet adapté aux précipitations de la zone tropicale africaine: Cas d’Adiopodoumé-Abidjan (Côte d’Ivoire). *Hydrol. Cont.* **1988**, *3*, 131–139.
50. Yao, F.Z.; Reynard, E.; Ouattara, I.; N’go, Y.A.; Fallot, J.-M.; Savané, I. A New Statistical Approach to Assess Climate Variability in the White Bandama Watershed, Northern Côte d’Ivoire. *ACS* **2018**, *8*, 410–430. [[CrossRef](#)]
51. Yao, K.C.J.; Kacou, M.; Koffi, E.S.; Dao, A.; Dutremble, C.; Guilliod, M.; Kamagaté, B.; Neppel, L.; Paturel, J.-E.; Perrin, J.-L.; et al. Rainfall Risk over the City of Abidjan (Ivory Coast): First Contribution to the Joint Analysis of Daily Rainfall from a Historical Record and a Recent Network of Rain Gauges. In Proceedings of the IAHS-AISH Scientific Assembly, Montpellier, France, 29 May–3 June 2022.
52. Balme-Debionne, M. Analyse Du Régime Pluviométrique Sahélien Dans Une Perspective Hydrologique et Agronomique: Étude de l’impact de Sa Variabilité Sur La Culture Du Mil. Ph.D. Thesis, Grenoble INPG, Grenoble, France, 2004.
53. Lawin, A. Analyse Climatologique et Statistique Du Régime Pluviométrique de La Haute Vallée de l’Oueme à Partir Des Données Pluviographiques Amma-Catch Benin. Ph.D. Thesis, Grenoble INPG, Grenoble, France, 2007.
54. Amouin, J.; Kouadio, K.Y.; Kacou, M.; Djakouré, S.; Ta, S. Diagnosis of the Causes of the Rain Flooding in June in the West Africa Coastal Area. *Atmos. Clim. Sci.* **2020**, *11*, 11–31. [[CrossRef](#)]

55. Houze, R.A., Jr. Convective and Stratiform Precipitation in the Tropics. In *Tropical Rainfall Measurements*; Theon, J.S., Fugono, N., Eds.; Deepak Pub.: Hampton, VA, USA, 1988; pp. 27–35.
56. Evaristo, R.; Scialom, G.; Viltard, N.; Lemaître, Y. Polarimetric Signatures and Hydrometeor Classification of West African Squall Lines. *Q. J. R. Meteorol. Soc.* **2010**, *136*, 272–288. [[CrossRef](#)]
57. Depaetere, C.; Gosset, M.; Ploix, S.; Laurent, H. The Organization and Kinematics of Tropical Rainfall Systems Ground Tracked at Mesoscale with Gages: First Results from the Campaigns 1999–2006 on the Upper Ouémé Valley (Benin). *J. Hydrol.* **2009**, *375*, 143–160. [[CrossRef](#)]
58. Maranan, M. Rainfall Types over Southern West Africa: Diagnosis, Synoptic Environments and Representation in Satellite Retrievals. Available online: <https://publikationen.bibliothek.kit.edu/1000099241> (accessed on 10 September 2020).
59. Maranan, M.; Fink, A.H.; Knippertz, P. Rainfall Types over Southern West Africa: Objective Identification, Climatology and Synoptic Environment. *Q. J. R. Meteorol. Soc.* **2018**, *144*, 1628–1648. [[CrossRef](#)]
60. Camberlin, P.; Kpanou, M.; Roucou, P. Classification of Intense Rainfall Days in Southern West Africa and Associated Atmospheric Circulation. *Atmosphere* **2020**, *11*, 188. [[CrossRef](#)]
61. Nel, W.; Hauptfleisch, A.; Sumner, P.D.; Boojhawon, R.; Rughooputh, S.D.D.V.; Dhurmea, K.R. Intra-Event Characteristics of Extreme Erosive Rainfall on Mauritius. *Phys. Geogr.* **2016**, *37*, 264–275. [[CrossRef](#)]
62. Gaye, A.; Viltard, A.; de Félice, P. Squall Lines and Rainfall over Western Africa during Summer 1986 and 87. *Meteorol. Atmos. Phys.* **2005**, *90*, 215–224. [[CrossRef](#)]
63. Sangiorgio, M.; Barindelli, S. Spatio-Temporal Analysis of Intense Convective Storms Tracks in a Densely Urbanized Italian Basin. *IJGI* **2020**, *9*, 183. [[CrossRef](#)]
64. Janiga, M.A.; Thorncroft, C.D. Convection over Tropical Africa and the East Atlantic during the West African Monsoon: Regional and Diurnal Variability. *J. Clim.* **2014**, *27*, 4159–4188. [[CrossRef](#)]
65. Zhang, G.; Cook, K.H.; Vizy, E.K. The Diurnal Cycle of Warm Season Rainfall over West Africa. Part I: Observational Analysis. *J. Clim.* **2016**, *29*, 8423–8437. [[CrossRef](#)]
66. Lafore, J.-P.; Flamant, C.; Giraud, V.; Guichard, F.; Knippertz, P.; Mahfouf, J.-F.; Mascart, P.; Williams, E.R. Introduction to the AMMA Special Issue on ‘Advances in Understanding Atmospheric Processes over West Africa through the AMMA Field Campaign. *Q. J. R. Meteorol. Soc.* **2010**, *136*, 2–7. [[CrossRef](#)]
67. Thorncroft, C.D.; Nguyen, H.; Zhang, C.; Peyrillé, P. Annual Cycle of the West African Monsoon: Regional Circulations and Associated Water Vapour Transport. *Q. J. R. Meteorol. Soc.* **2011**, *137*, 129–147. [[CrossRef](#)]
68. Raj, J.; Bangalath, H.K.; Stenchikov, G. West African Monsoon: Current State and Future Projections in a High-Resolution AGCM. *Clim. Dyn.* **2019**, *52*, 6441–6461. [[CrossRef](#)]

Disclaimer/Publisher’s Note: The statements, opinions and data contained in all publications are solely those of the individual author(s) and contributor(s) and not of MDPI and/or the editor(s). MDPI and/or the editor(s) disclaim responsibility for any injury to people or property resulting from any ideas, methods, instructions or products referred to in the content.